ISSN 0023-1584, Kinetics and Catalysis, 2014, Vol. 55, No. 6, pp. 809–823. © Pleiades Publishing, Ltd., 2014.

The Use of Boric Acid (H_3BO_3) and Boron Oxide (B_2O_3) for Co-Precipitation Synthesis of Cobalt–Boron Catalysts: Catalytic Activity in Hydrogen Generation[1]

B. Coşkuner[a], A. Kantürk Figen[a,*] and M. B. Pişkin[b]

[a] *Department of Chemical Engineering, Yildiz Technical University, Istanbul 34210, Turkey*

[b] *Department of Bioengineering, Yildiz Technical University, Istanbul 34210, Turkey*

**e-mail: akanturk@yildiz.edu.tr; ayselkanturk@gmail.com.tr*

Received March 21, 2014

Abstract—The use of boric acid (H_3BO_3) and boron oxide (B_2O_3) for the synthesis of cobalt-based catalysts by the co-precipitation technique was investigated and catalytic activities in hydrogen generation were evaluated. Different cobalt salts [cobalt (II) chloride ($CoCl_2 \cdot 6H_2O$), cobalt sulfate ($CoSO_4 \cdot 5H_2O$) and cobalt(II) nitrate ($Co(NO_3)_2 \cdot 7H_2O$)] were used with H_3BO_3 and B_2O_3 to prepare Co based catalysts. Crystalline, surface and chemical characteristics were clarified using X-ray diffraction (XRD); low temperature adsorption of nitrogen (BET), scanning electron microscopy (SEM), and inductively coupled plasma optical emission spectroscopy (ICP–OES). Three types of powder samples were obtained according to the different boron sources and cobalt salts, and it was found that an efficient Co based catalyst was obtained by co-precipitation of B_2O_3 and $CoCl_2 \cdot 6H_2O$ salt. Additionally, the effect of temperature, stabilizer ratio and $NaBH_4$/catalyst ratio on parameters, characterizing the reaction of hydrogen generation was investigated. The zero order, first order and Langmuir–Hinshelwood kinetic models were used to identify the effect of Co based catalysts on the behavior of the catalytic system in hydrogen generation. Kinetic parameters of hydrogen generation for zero-order kinetic model were calculated for the following conditions: the rate of hydrogen generation is 0.93 L H_2 g^{-1}catalyst min^{-1}, the activation energy is 43.55 kJ mol^{-1} and the constant of Arrhenius equation is 11 min^{-1}.

DOI: 10.1134/S002315841466001X

INTRODUCTION

Technical progress and rapidly growing world population lead to increasing energy consumption. Owing to the effect of global warming and depletion of fossil flues hydrogen is considered as an important fuel for future energy needs. Although hydrogen gas (H_2) is a promising energy carrier, the storage of the generated hydrogen is one of the main challenges on the way to the hydrogen economy. Due to its non-toxic nature, environmental safety, abundance on earth, feasibility of production, hydrogen is recognized as an energy source competing with fossil fuels. Current hydrogen storage technologies involve hydrogen compression, production of liquid hydrogen, use of porous solid adsorbents and metal hydrides [1, 2]. For vehicular applications, the US Department of Energy (DOE) has set storage targets; the gravimetric (volumetric) system targets for near-ambient temperature (from 40 to 85°C) and moderate pressure (less than 100 bar) is 9.0 wt % (81 g/L) for 2015 [3]. Among various hydrogen storage materials, chemical hydrides have been regarded as the most promising solids for hydrogen supply and storage due to their capability to supply ultrapure H_2 and larger H_2 storage capacity [4, 5].

Hydrogen generation from the hydrolysis reaction of an alkaline sodium borohydride ($NaBH_4$) solution has drawn much attention due to its theoretically high hydrogen storage capacity (11 wt %). Hydrolysis of $NaBH_4$ proceeds according to the following reaction:

$$NaBH_4 + (2 + x)H_2O \longrightarrow NaBO_2 \cdot xH_2O + 4H_2. \quad (1)$$

The hydrolysis reaction of $NaBH_4$ is efficient to yield 4 mol H_2/mol $NaBH_4$ i. The x (mole of water) is generally 2 in the reaction [1, 2]. Moreover, $NaBH_4$ is self-decomposable in aqueous solution and it can be stabilized by alkalization. A catalyst is needed to accelerate the hydrogen release [6, 7]. Nowadays, the search for an efficient catalyst for $NaBH_4$ hydrolysis remains to be an important issue.

Acids, metal complexes, salts, alloys and supported catalysts are developed to achieve hydrogen production in the highest yield. Metal-based catalysts (such as Fe, Co, Ni, Cu, Ru, Rh, Pt, Pd , Ir) attracted significant attention, among these Co shown the highest activity in hydrolysis of $NaBH_4$. Co catalysts are preferred since they are highly active for hydrogen generation and inexpensive. To improve surface properties of Co metal and form Co containing active phase, Co

[1] The article is published in the original.

Table 1. The Co based catalysts via co-precipitation synthesis in this study

Code	Cobalt source	Boron source
B/Co–1	$CoCl_2 \cdot 6H_2O$	H_3BO_3
B/Co–2		B_2O_3
B/Co–3	$CoSO_4 \cdot 5H_2O$	H_3BO_3
B/Co–4		B_2O_3
B/Co–5	$Co(NO_3)_2 \cdot 6H_2O$	H_3BO_3
B/Co–6		B_2O_3

based /alloys/supported catalysts rather than metal Co are used.

Earlier, Co based/alloys/supported catalysts were prepared by chemical reduction [5, 8] and sol–gel methods [9]. Although different methods to prepare Co–B catalysts were described, the use of H_3BO_3 and B_2O_3 for preparation of Co–B catalysts by co-precipitation technique was not reported earlier. Recently, Shen et al. published paper on solvent effects in the synthesis of CoB catalysts via chemical reduction method. The authors indicated that CoB catalysts synthesized in different solvents showed very different surface areas, pore size distributions and pore volumes [10].

The main purpose of this study was to investigate H_3BO_3 and B_2O_3 as boron sources for co-precipitation synthesis of Co–B catalyst. Different cobalt salts [cobalt (II) chloride ($CoCl_2 \cdot 6H_2O$), cobalt sulfate ($CoSO_4 \cdot 5H_2O$) and cobalt (II) nitrate ($Co(NO_3)_2 \cdot 7H_2O$)] were used to prepare Co based catalysts via co-precipitation. Effect of temperature (22–60°C), the stabilizer ratio (1, 5, 10, 15 wt %) and the catalyst/$NaBH_4$ ratio (0.03, 0.05, 0.11, 0.21 wt/wt) on parameters characterizing the generation of hydrogen from $NaBH_4$ solution (0.12 M) was investigated. Additionally, kinetic investigation was performed to evaluate equations describing the hydrogen generation rate using zero-order, first-order, and Langmuir–Hinshelwood kinetic models.

MATERIALS AND METHODS

Materials

H_3BO_3 (99%) and B_2O_3 (99%) used as boron source were purchased from Eti Mine Works General Management-Turkey; $CoCl_2 \cdot 6H_2O$ (97%), $CoSO_4 \cdot 7H_2O$ (97%) and, $Co(NO_3)_2 \cdot 6H_2O$ (99%), used as cobalt salts were procured from Merck; sodium hydroxide (NaOH, Labor Technic), used as stabilizer, and $NaBH_4$ (96%) used as hydrogen storage medium were purchased from Fluka.

Preparation of Co Based Catalysts by Co-Precipitation

Co based catalysts were prepared via co-precipitation from different boron source and cobalt salts and obtained catalysts were designated as given in Table 1. Firstly, 0.5 M boron solution was prepared and then cobalt sources were added. This obtained solution was mixed for 2 h at 85 ± 3°C with magnetic stirring (500 rpm) for produce bulk structure. Bulk materials were then dried at ≈100°C under vacuum overnight to eliminate the excess water. To promote formation of the stable structure catalysts were calcined at 500°C for 4 h. In this way six Co based catalysts were obtained, stored in inert atmosphere and then the characterization and hydrogen generation reaction were performed. These catalysts were activated in H_2 before the generation tests.

Characterization

Crystalline, surface and chemical characteristics were obtained using X-ray diffraction (**XRD**), Brunauer–Emmett–Teller (**BET**) N_2 adsorption measurements and scanning electron microscopy (**SEM**), and inductively coupled plasma optical emission spectroscopy (**ICP–OES**).

XRD analysis. X-ray diffraction was used to identify the structure of Co based catalysts and the materials required for the synthesis (Figs. 1, 2). The X-ray analysis was carried out at ambient temperature with a Philips Panalytical X'Pert-Pro diffractometer using CuK_α radiation ($\lambda = 0.15418$ nm) at 40 mA and 45 kV with a step size of 0.02° and a speed of 1° (2°) per min. The diffractorams were compared with inorganic crystal structure database (**ICSD**) references for identification purposes (Table 2).

BET analysis. The specific surface areas of Co based catalysts were measured using the Brunauer–Emmett–Teller (Quantachrome) analysis by adsorbing N_2 with multipoint modes (Table 3). The catalysts were degassed at 500°C overnight.

SEM analysis. Microstructure studies of the Co based catalysts were performed using a JEOL (JSM 5410 LV) scanning electron microscope (Fig. 3). The sample was covered with Au and made ready for analysis by fixing the sample on the sample holder with a carbon sticky band.

ICP–OES analysis. The elemental analysis of Co based catalyst was performed using an ICP–OES (Perkin Elmer, Optima 2100 DV). To prepare samples for analysis, the material was digested in a hydrochloric acid/nitric acid/hydrofluoric acid/phosphoric acid ($HCl/HNO_3/HF/H_3PO_4$) solution. The samples were analyzed at least three times and mean values were used as one observation.

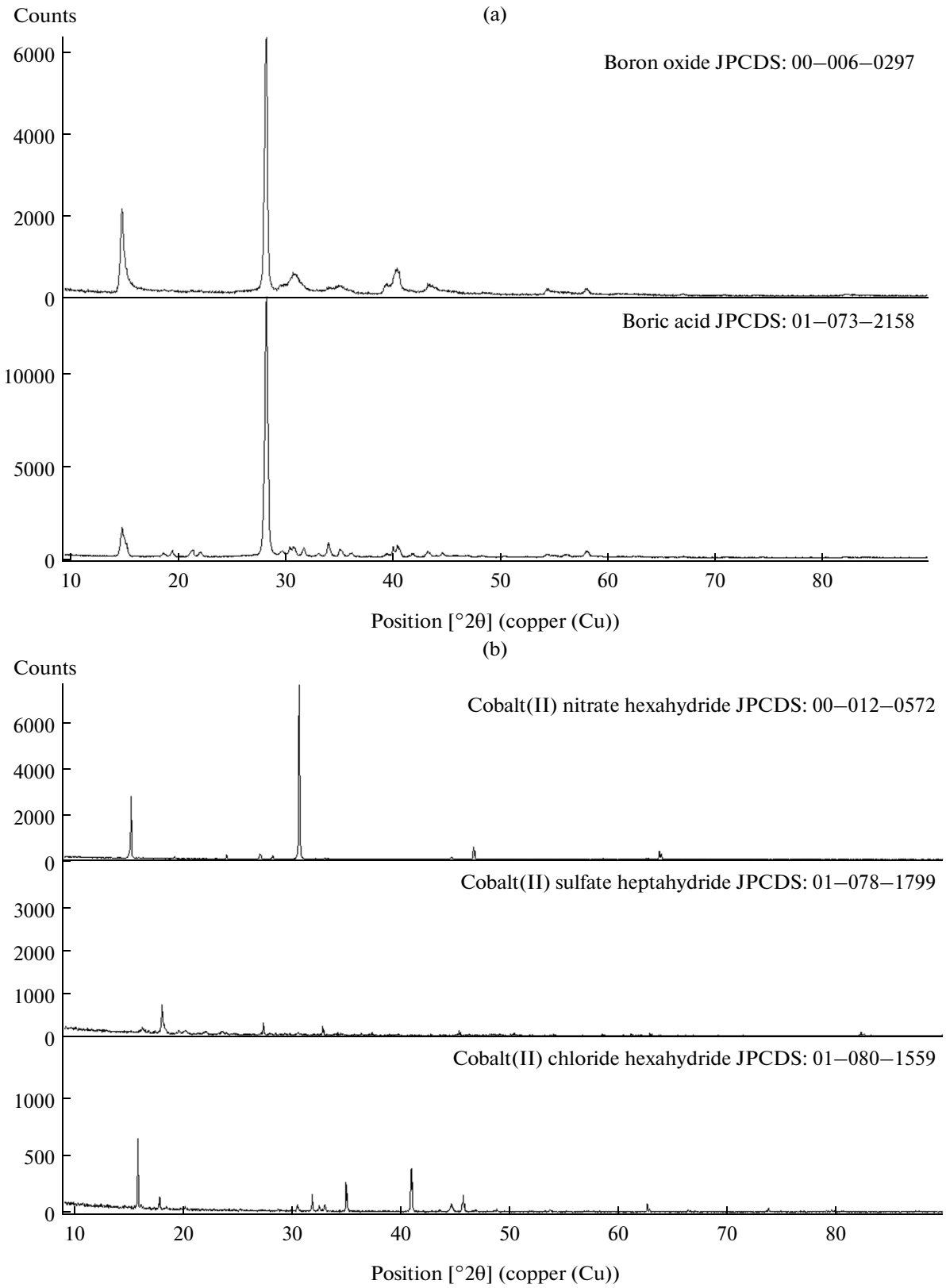

Fig. 1. The XRD patterns of compounds used to prepare Co based catalysts: (a) boron sources, (b) cobalt salts.

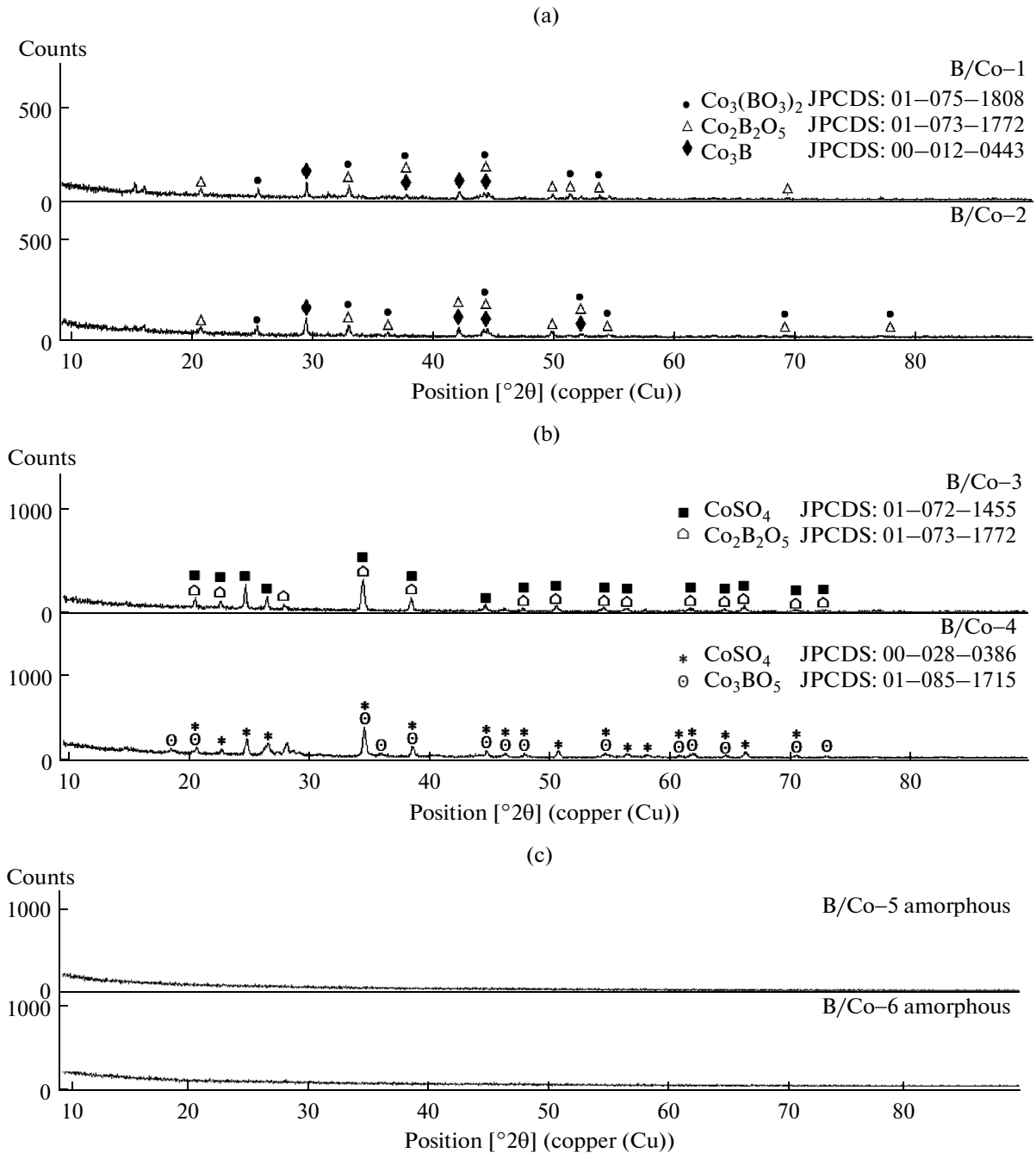

Fig. 2. The XRD patterns of Co based catalysts synthesized by co-precipitation: a—B/Co–1 and B/Co–2; b—B/Co–3 and B/Co–4; c—B/Co–5 and B/Co–6.

Hydrogen Generation Tests

Hydrogen generation tests were performed in the presence of Co based catalysts in alkaline $NaBH_4$ solution in micro reactor. A 15 mL glass reactor was used to conduct the hydrolysis and evaluate the activity of Co based catalysts. Outlet of the reactor was connected with a piece of rubber hose to transfer the evolved hydrogen to the water-filled inverted burette to measure the generated H_2 volume during the hydrolysis. The water displacement method was used for scaling the quantity of generated hydrogen. Activation energy and reaction order of $NaBH_4$ hydrolysis reaction were estimated in the presence of Co based catalyst. The sampling was made at different intervals of times and the relevant data were fitted with ideal reaction kinetic model that has the proximately coeffient of cofactor.

Table 2. The crystalline phase properties of Co based catalysts

Catalyst	Phases	JPCDS	*I*, %	2θ,°	*h k l*
B/Co–1	Co_3B	00–012–0443	100.00	45.912	1 0 3
			98.40	44.577	2 1 0
			53.80	46.738	2 1 1
	$Co_3(BO_3)_2$	01–075–1808	100.00	33.315	1 2 1
			48.40	39.972	2 1 1
B/Co–2			40.60	22.261	1 3 0
	$Co_2B_2O_5$	01–073–1772	100.00	33.315	−1 0 2
			98.40	39.972	0 1 1
			53.80	22.261	1 0 2
B/Co–3	$CoSO_4$	01–072–1455	100.00	34.404	1 1 2
			83.00	34.467	2 0 0
			66.30	24.632	1 1 1
	$Co_2B_2O_5$	01–073–1772	100.00	34.654	−1 0 2
			98.40	20.433	0 1 1
			53.80	35.572	1 0 2
B/Co–4	$CoSO_4$	00–028–0386	100	34.399	2 1 1
			65	24.641	1 1 1
			45	26.442	1 2 0
	Co_3BO_5	01–085–1715	100.00	35.387	2 0 1
			78.2	35.302	2 4 0
			50.3	17.441	1 2 0
B/Co–5	Amorphous				
B/Co–6					

Table 3. The texture properties of Co based catalysts

Catalyst	Surface area, $m^2\ g^{-1}$	SEM		
		average particle size, μm	minimum particle size, μm	maximum particle size, μm
B/Co–1	9.1870	6	2.8	39
B/Co–2	10.6300	3	2.85	25
B/Co–3	0.3982	148	7	357
B/Co–4	0.5795	750	1285	1500
B/Co–5	0.8691	1.7	0.714	3
B/Co–6	0.7419	58	7	178

Hydrogen generation was performed based on two experimental procedures. The first procedure aimed at finding the best catalyst was characterized by the highest rate of hydrogen production. The experiments were conducted under following conditions: catalyst/$NaBH_4$ = 0.11 wt/wt, 40°C, 10 wt % NaOH, 0.12 M $NaBH_4$ and 400 rpm. In the second procedure, hydrogen production (Fig. 4) was investigated as a function of temperature (22, 40 and, 60°C), NaOH/catalyst ratio (1, 5, 10 and, 15 wt %) and $NaBH_4$/catalyst (0.03, 0.05, 0.11, 0.21 wt/wt) ratio (Fig. 5).

When the reaction of hydrogen production conducted under optimum conditions was completed, the catalysts were analyzed by XRD to determine changes in the structure (Fig. 6). The used catalysts were filtered from the solution and washed three times with water and ethanol followed by drying at 105°C for 24 h.

Hydrogen Generation Kinetics

Measurements of the specific surface area and structure indicated that the B/Co–2 sample was a

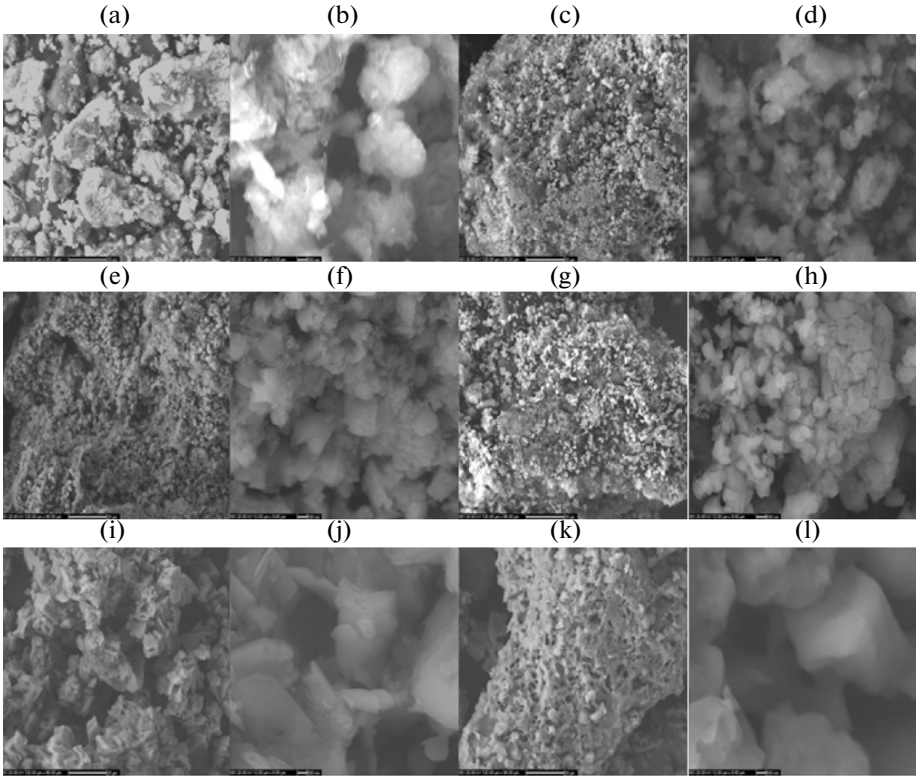

Fig. 3. The SEM morphology of Co based catalysts. B/Co–1: ×1000 (a), ×10000(b); B/Co–2: ×1000 (c), ×10000 (d); B/Co–3: ×1000 (e), ×10000 (f); B/Co–4: ×1000 (g), ×10000 (h); B/Co–5: ×1000 (i), ×10000 (j); B/Co–6: ×1000 (k), ×10000 (l).

preferable material for catalytic teats. Accordingly, kinetics of hydrogen production was conducted in the presence of the B/Co–2 catalyst. Hydrogen production was performed under following conditions: catalyst/$NaBH_4$ was 0.11 wt /wt, 22, 40 and, 60°C, stabilizer ratio was 10 wt %, 0.12 M $NaBH_4$ solution (Fig. 7).

Kinetic analysis was made using hydrogen production rates and the $NaBH_4$ concentrations as a function of time. To construct a kinetic model, zero-order, first-order rate, and Langmuir–Hinshelwood kinetic models were examined by least-square method. The coefficient of correlation of the all reaction orders was calculated to find reaction order as shown in Table 4.

Considering the behavior of reaction three different kinetic models were applied for kinetic analysis. The zero order kinetics is independent of any reactant concentration and does not involve assuming the kinetic model:

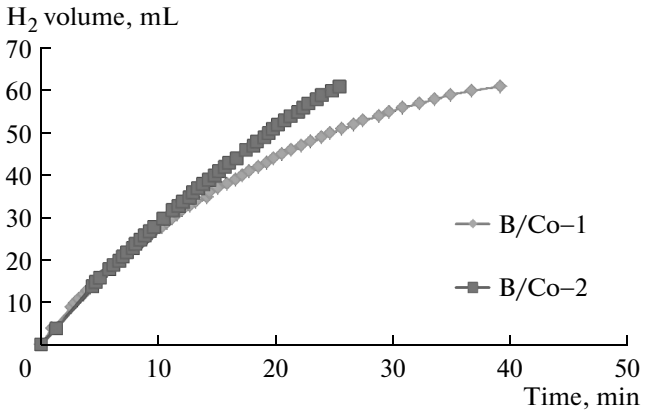

Fig. 4. The volume of hydrogen produced in the presence of the Co based catalyst at 40°C, 10 wt % NaOH, 0.12 M $NaBH_4$ solution.

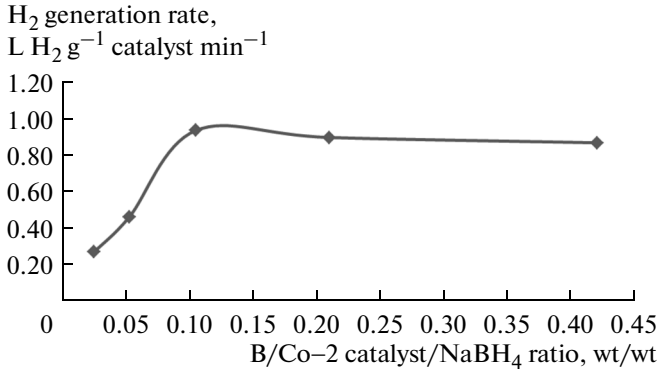

Fig. 5. Effect of the catalyst amount on the rate of hydrogen generation for the Co based catalyst at 40°C, 10 wt % NaOH, 0.12 M $NaBH_4$ solution.

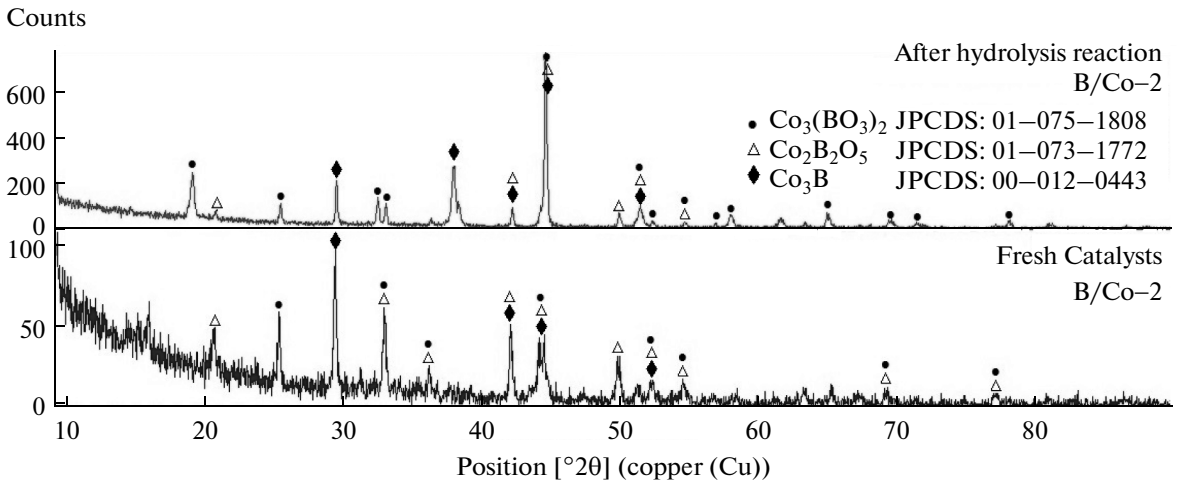

Fig. 6. The XRD patterns of B/Co–2 catalysts recorded for fresh catalysts and for catalysts used in hydrolysis reaction.

$$dC_{NaBH_4}/dt = -r_{NaBH_4} = -k(T). \quad (2)$$

Where C_{NaBH_4} is the concentration, r is the rate of reaction, k is the reaction rate constant based on the solution volume. A plot of $(C_{NaBH_{40}} - C_{NaBH_4})$ as a function of time was found to be be linear with slope giving the reaction rate constant. For all kinetic models values of the activation energies (E_a) were calculated from the Arrhenius equation (Fig. 8). After determining the reaction order a slope of the plot of Arrhenius equation gives E_a for the catalytic hydrolysis of $NaBH_4$ with its intercept as the Arrhenius constant (k_0).

In the first-order kinetic model, the reaction rate depends on the reactant concentration and, an integrated form of this model is described by the equation (3)

$$\ln\left(\frac{C_{NaBH_{4_0}}}{C_{NaBH_4}}\right) = -k(T)t. \quad (3)$$

The hydrogen generation from $NaBH_4$ in the presence of Co–B catalysts is a liquid phase reaction occurring on a solid catalysts surface. The Langmuir–Hinshelwood model is conventionally used to explain the features of catalytic reactions (Fisg. 9, 10). The model, is as seen above Eq. (4), was applied the data using calculated values of the adsorption constant, K_a. This constant could be determined by minimizing the

Table 4. Coefficient of correlation of zero, first order reaction and Langmuir–Hinshelwood kinetics model of $NaBH_4$ hydrolysis by B/Co–2.

Concentration of NaOH, wt %	Temperature, °C	Zero-order	First-order	Langmuir–Hinshelwood
1	22	0.9973	0.8094	0.9995
	40	0.9927	0.8305	0.9989
	60	0.9797	0.8728	0.9939
5	22	0.9906	0.8516	0.9992
	40	0.9894	0.8562	0.9987
	60	0.9761	0.8960	0.9902
10	22	0.9824	0.8665	0.9973
	40	0.9935	0.8495	0.9993
	60	0.9965	0.7894	0.9993
15	22	0.9783	0.8837	0.9957
	40	0.9806	0.8785	0.9978
	60	0.9964	0.7983	0.9993

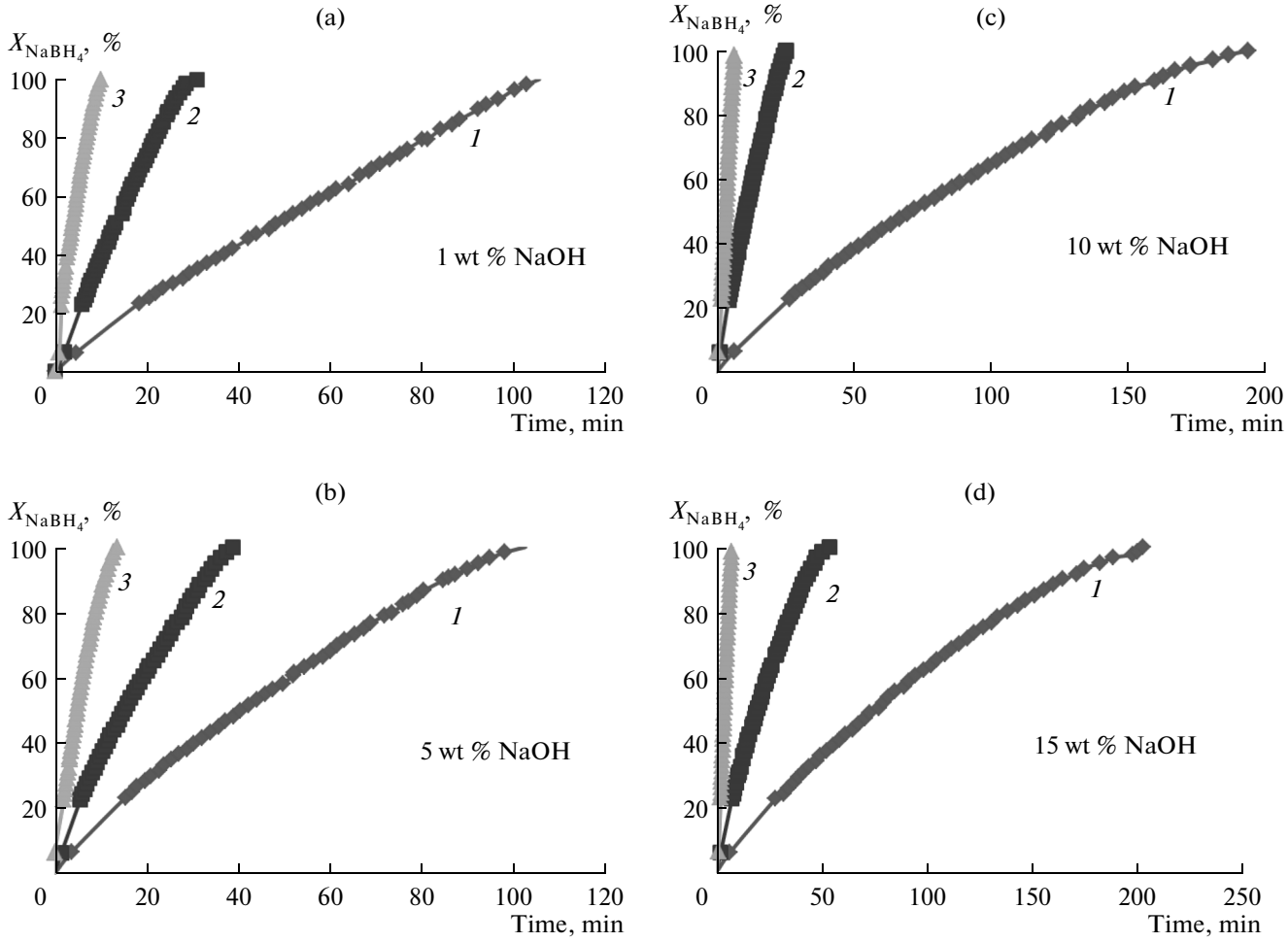

Fig. 7. Hydrogen generation yield versus time at temperatures of 22 (*1*), 40 (*2*), 60 (*3*) °C and at concentrations of NaOH 1 (a), 5 (b), 10 (c), and 15 (d) wt % with 0.12 M $NaBH_4$.

objective function (Eq. 5) of the correlation coefficients for data obtained at 40 and 60°C [11–13].

$$\frac{1}{K_a}\ln\left(\frac{C_{NH_3BH_{3_0}}}{C_{NH_3BH_3}}\right) + (C_{NH_3BH_{3_0}} - C_{NH_3BH_3}) = kt, \quad (4)$$

$$\min_{K_a} f(K_a) = (1 - R^2_{40°C}) + (1 - R^2_{60°C}). \quad (5)$$

RESULTS AND DISCUSSION

Characterization of Co-based Catalysts

Figure 1 shows the XRD patterns of cobalt compounds used for the catalyst preparation ($CoCl_2 \cdot 6H_2O$, $CoSO_4 \cdot 7H_2O$, $Co(NO_3)_2 \cdot 6H_2$ along with H_3BO_3 and B_2O_3 used as the boron source. XRD patterns of H_3BO_3 showed peaks characteristic of anorthic structure taken from 01–073–2158 JPCDS whereas cubic crystalline structure could be identified for B_2O_3 according to 00–006–0297 JPCDS (Fig. 1a). $CoCl_2 \cdot 6H_2O$ and $CoSO_4 \cdot 5H$ 2O showed monoclinic structure according to 01–080–1559 and 01–078–1799 JPCDS, respectively. The JPCDS number for $Co(NO_3)_2 \cdot 6H_2O$ is 00–012–0572 (Fig. 1b).

Figure 2 shows the XRD patterns of obtained six powders after the co-precipitation and calcination at 500°C with crystalline phase properties of powders listed in Table 2. As can be seen three types of powders were obtained according to the variety of boron sources and cobalt salts used in co-precipitation synthesis. Depending on the crystal properties the powders can be divided into crystalline (B/Co–1, B/Co–2), unformed (B/Co–3, B/Co–4) and, amorphous (B/Co–5, B/Co–6).

Figure 2a shows the XRD patterns of B/Co–1 and B/Co–2 samples. As can be seen two samples show the same crystal phase properties (Table 2). Based on characteristic XRD peaks shown by the catalysts Co_3B, $Co_2B_2O_5$ and $Co_3(BO_3)_2$ along with cobalt boride phases could be identified. No diffraction peaks corresponding to other boron or cobalt compounds could be found. As a result, Co–B structure was formed when H_3BO_3 and B_2O_3 were co-precipitation

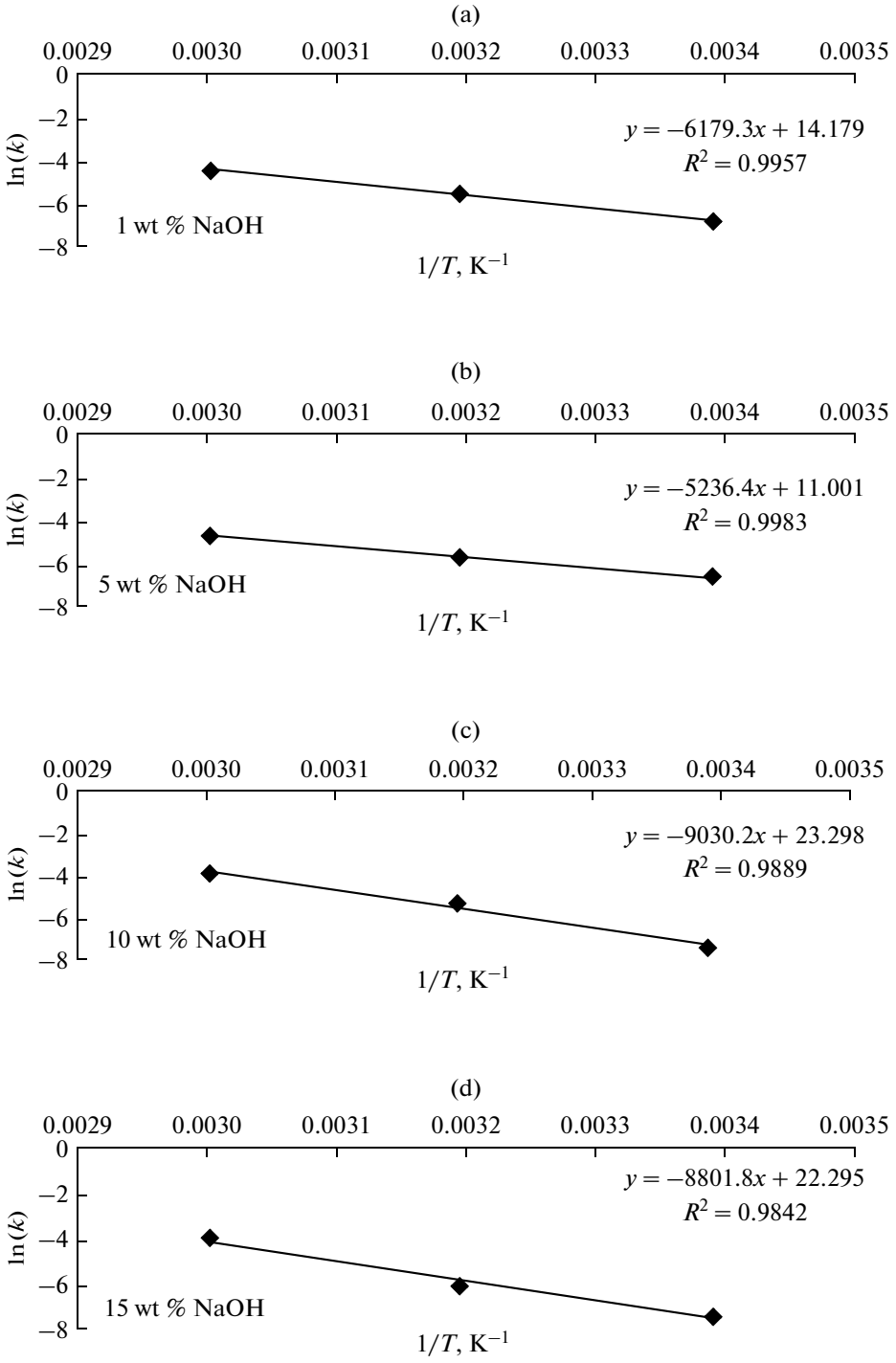

Fig. 8. Arrhenius plot for hydrolysis of 0.12 M $NaBH_4$ in solutions containing 1 (a), 5 (b), 10 (c), and 15 (d) wt % NaOH.

with $CoCl_2 \cdot 6H_2O$ salt and Co–B catalysts were synthesized via co-precipitation synthesis successfully.

Figure 2b shows the XRD patterns of B/Co–3 and B/Co–4 samples prepared from H_3BO_3 and B_2O_3 respectively co-precipitated with $CoSO_4 \cdot 5H_2O$ salt. Though, $Co_2B_2O_5$ in the crystalline structure was formed, $CoSO_4$ was also found in the crystalline structure of B/Co–3. Consequently, a phase with the structure of Co_3BO_5 along with admixture of unconsummated $CoSO_4$ could be also found in the B/Co–4 sample. When $CoSO_4 \cdot 7H_2O$ salt was used, the crystalline structure of $CoSO_4$ was partially transformed into the Co–B structure (Table 2). The nature of boron sources did not affect the extent of the transfor-

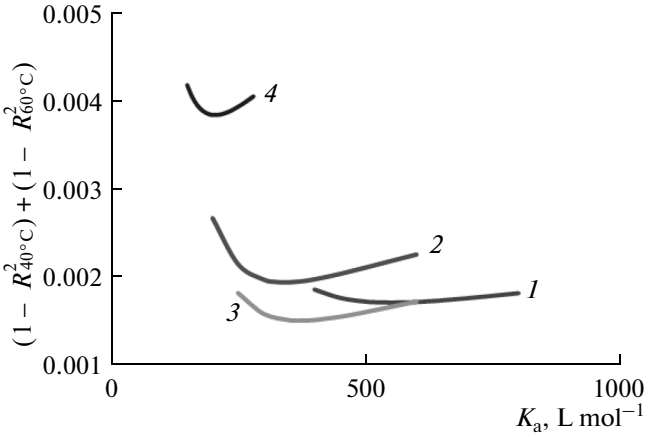

Fig. 9. Determination of the adsorption constant for Langmuir–Hinshelwood by using the data at 40 and 60°C for model developed for hydrolysis of 0.12 M $NaBH_4$ in solutions containing 1 (*1*), 5 (*2*), 10 (*3*), and 15 (*4*) wt % NaOH.

mation to Co–B structure, however it affected the crystalline structure of the Co–B–O phase.

Figure 2c shows the XRD patterns of the B/Co–5 and B/Co–6 samples. The figure indicates, that synthesis from H_3BO_3 and B_2O_3 by co-precipitation with $Co(NO_3)_2 \cdot 6H_2O$ salt results in an amorphous to X-rays phase. When $Co(NO_3)_2 \cdot 6H_2O$ salt was used in the co-precipitation synthesis unformed crystalline phase was yielded independently of boron source.

With the co-precipitation process, the interaction of cobalt ions with borate anions takes place resulting in the cobalt borate. In this work the crystalline cobalt boride phases were identified as Co_3B, $Co_2B_2O_5$, and $Co_3(BO_3)_2$. Also the catalysts could contain some amount of amorphous cobalt-containing phase and typical amorphous CoB peak at around 45°(2θ). The synthesized catalyst was very active in the $NaBH_4$ hydrolysis due to the presence of active cobalt-boron containing phase such as cobalt boride. Furthermore, sodium metaborate ($NaBO_2$) has a negative influence on the H_2 generation rate [14].

Figure 3 shows the SEM image of six Co based powders made with magnification 1000 x and 10000 x. SEM observation indicated a wide particle-size distribution in catalysts (Table 3). Morphology of Co based powders was significantly affected by the nature of boron sources and cobalt salts. Examination of B/Co–1 and B/Co–2, which were prepared by co-precipitation of H_3BO_3 and B_2O_3 respectively with $CoCl_2 \cdot 6H_2O$ salt, showed a strong impact of boron sources on their morphology and size distribution. B/Co–1 had a heterogeneous particle-size distribution, while B/Co–2 showed a more homogeneous distribution. The powder samples of B/Co–3 and B/Co–4 synthesized by co-precipitation H_3BO_3 and B_2O_3 with $CoSO_4 \cdot 7H_2O$ salt had nanosized structures with micrometer size clusters. B/Co–5 and B/Co–6 produced from $Co(NO_3)_2 \cdot 6H_2O$ salt by co-precipitation with H_3BO_3 and B_2O_3 respectively differ in morphological structure from other samples (Fig. 3). The reason may lie in the presence of an amorphous phase.

Moreover, the specific surface areas of B/Co and B/Co–2 catalysts produced from $CoCl_2 \cdot 6H_2O$ and B_2O_3 had the largest surface area (10.63 $m^2 g^{-1}$) among catalysts studied. It appears that results of SEM and BET measurements are in good agreement.

Based on texture and crystalline properties B/Co–2 catalyst was found to be the most suitable for hydrogen production. In addition to this, the obtained B/Co–2 was analyzed by ICP–OES spectroscopy to clarify the chemical composition. The results of ICP–OES showed that the Co content in the B/Co catalyst was 21.99 wt % and that of B was14.08 wt %.

Hydrogen Generation Tests

Figure 4 shows that the volume of hydrogen generated as a function of reaction time for B/Co–1 and B/Co–2 catalysts. Hydrogen generation experiments were performed under following conditions: catalyst/$NaBH_4$ = 0.11 wt/wt, 40°C, 10 wt % NaOH, 0.12 M $NaBH_4$, and 400 rpm.

For two types of Co based catalysts, H_2 liberation followed a regular trend. Reaction time was taken to be 24.8 min in the presence of B/Co–1 while 39.18 min. was chosen on using B/Co–2. In addition, hydrogen generation rate was calculated as 0.62 L H_2 g^{-1} catalyst min^{-1} for B/Co–1 catalyst and 0.93 L H_2 g^{-1} catalyst min^{-1} for B/Co–2 catalyst. It can be seen that B/Co–2 with the largest surface area was more active than B/Co–1 in hydrogen production from alkaline $NaBH_4$ solution. The data for B/Co–2 indicated that in the presence of this catalyst the highest rate of hydrogen production with 100% of the theoretical H_2 yield was observed. For this reason, B/Co–2 was selected for kinetic investigations.

Effect of Catalyst/$NaBH_4$ Ratio on Hydrogen Generation

Figure 5 shows the effect of the B/Co–2 catalyst/$NaBH_4$ ratio on the rate of hydrogen production in 0.12 M $NaBH_4$ solution at 40°C. The rate of hydrogen production in the presence of the B/Co–2 catalyst was calculated for catalyst/$NaBH_4$ ratios of 0.03, 0.05, 0.11, 0.21 and 0.42 wt/wt Reaction times were determined as 352.13 min. 97.71, 24.80, 13.28 and, 7.33 min. respectively. As the B/Co–2 catalyst/$NaBH_4$ ratio was increased from 0.03 to 0.11, H_2 generation rate increased 3.44 times. Although, B/Co–2 catalyst/$NaBH_4$ ratio was increased from 0.11 to 0.42, no significant change in hydrogen generation was observed. Based on the value of hydrogen generation rate and reaction time the 0.11 B/Co–2 catalyst/$NaBH_4$ ratio appears to be the optimal ratio for this study.

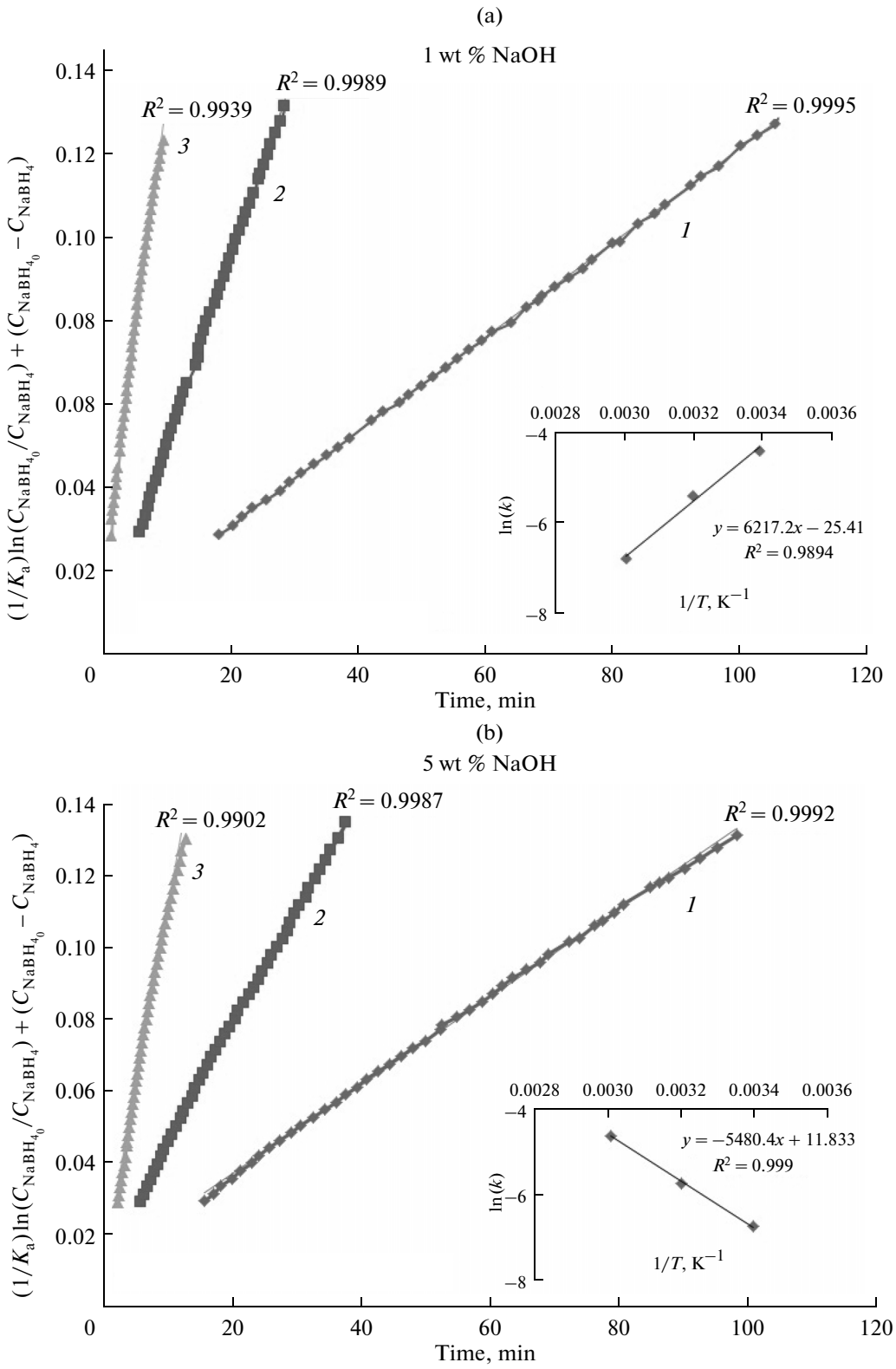

Fig. 10. Langmuir–Hinshelwood kinetic model for hydrolysis of 0.12 M $NaBH_4$ in solutions containing 1 (a), 5 (b), 10 (c), and 15 (d) wt % NaOH: *1*—22, *2*—40 and *3*—60°C.

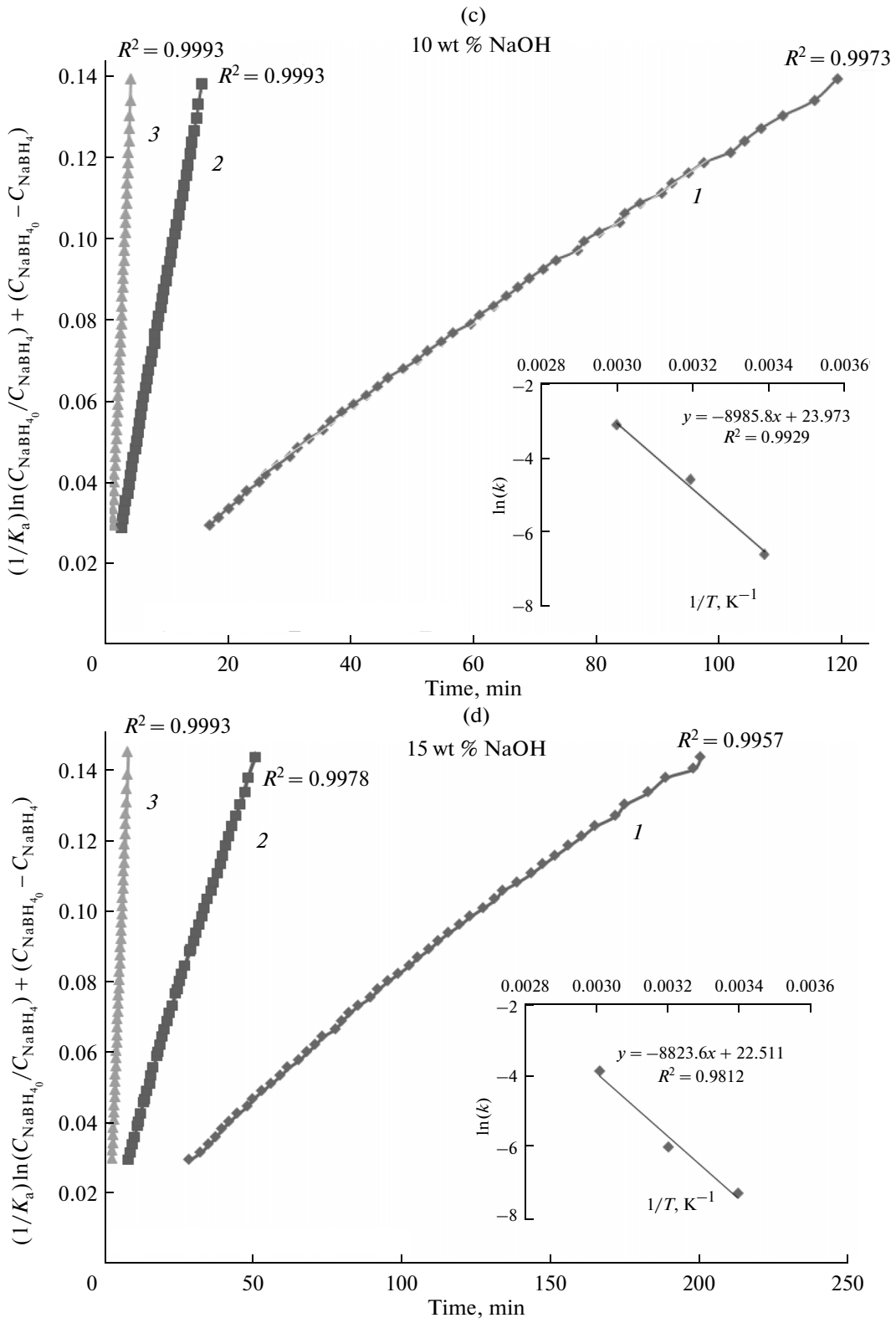
(c)
10 wt % NaOH
$R^2 = 0.9993$
$R^2 = 0.9993$
$R^2 = 0.9973$
3
2
1
$(1/K_a)\ln(C_{NaBH_{4_0}}/C_{NaBH_4}) + (C_{NaBH_{4_0}} - C_{NaBH_4})$
Time, min
$y = -8985.8x + 23.973$
$R^2 = 0.9929$
ln(k)
1/T, K^{-1}
(d)
15 wt % NaOH
$R^2 = 0.9993$
$R^2 = 0.9978$
$R^2 = 0.9957$
3
2
1
$(1/K_a)\ln(C_{NaBH_{4_0}}/C_{NaBH_4}) + (C_{NaBH_{4_0}} - C_{NaBH_4})$
Time, min
$y = -8823.6x + 22.511$
$R^2 = 0.9812$
ln(k)
1/T, K^{-1}

Fig. 10. (Contd.)

Table 5. Activation energies of $NaBH_4$ hydrolysis by Co based catalysts

Catalyst	Synthesis method	NaOH, wt %	Activation energy, kJ mol^{-1}	References
CoB amorphous	Chemical reduction	5	64.87	[5]
5 wt % Co-αAl_2O_3	Impregnation	1	53.80	[23]
Amorphous Co/B	Solid state	1	48.07	[17]
C-supported Co–B	Impregnation-chemical reduction	–	57.80	[24]
Co_2B	In situ prepration	5	77.96–85.17	[25]
Co–Cu–B	Co-precipitation	7	49.60	[26]
Co–B	Chemical reduction	–	45.00	[18]
			51.37*	
B/Co	Co-precipitation	1	51.69**	This study
			43.55*	
B/Co	Co-precipitation	5	45.56**	This study
			75.07*	
B/Co	Co-precipitation	10	74.71**	This study
			73.18*	
B/Co	Co-precipitation	15	73.36**	This study

* E_a values is for zero-order kinetic model; ** E_a values is for Langmuir–Hinshelwood kinetic model.

As it is known from literature, amorphous cobalt boride catalysts are more active then crystalline systems. Cobalt based boron catalysts of this type are generally synthesized via chemical reduction method from $NaBH_4$ and various cobalt precursors with different calcination temperature are used to trace the effect of preparation conditions on the catalytic properties. Results of these studies indicated that the formation of crystalline structure depends on calcination temperature. In this study, we investigated different boron sources and synthesizing method for production of cobalt based boron catalysts. We selected calcination temperature as 500°C for investigating the effect of synthesizing method on the catalysts structure. In our earlier work [15] we were able to obtain amorphous catalysts at the same calcination conditions using different preparation procedure. When we increased the calcination temperature to 700°C in this protocol, structure became more crystalline. Based on our previous study we selected 500°C as a calcination temperature. When we compared B/Co–2 with Co based boron catalysts for hydrogen production from $NaBH_4$ at the same conditions (40°C 10 wt % NaOH) B/Co–2 catalysts showed a higher activity (0.93 L H_2 min^{-1} g^{-1}) than amorphous catalysts (0.84 L H_2 min^{-1} g^{-1}) [16]. In terms of hydrogen generation rate, crystalline B/Co–2 is as reactive as other catalysts described in literature. Hydrogen generation rates of 0.59 l, 0.681, 0.875, 0.032 and, 0.61 L H_2 min^{-1} g-cat^{-1} were reported for solid acidic Co–B [17], Co–B [18] Co, metallic Co [5], and 5 wt % Ru on IRA–400 [6] catalysts respectively.

After hydrogen generation tests, the XRD analysis was performed on the used B/Co–2 catalysts. For this analysis, the catalysts, which were used at optimum conditions (10 wt % NaOH, 40°C), were selected. Based on the XRD results, crystalline structures of fresh and used catalysts did not change significantly but crystallinity increased after hydrogen generation test. The active sites of Co based boron catalysts appear to be intermetallic cobalt compounds [14, 19, 20]. Catalyst could preserve amorphous phases of cobalt and after the hydrolysis reaction the crystallinity could change. Also, our catalyst may contain some amorphous phases since in our XRD pattern the peak near the 45°(2θ) occurred that can be attributed to the $Co_2B_2O_5$ and Co_3B crystalline phases. Amorphous phase of cobalt could not be determined by XRD in our study. For this reason we can not confirm that the increasing crystallinity is due to reduction of amorphous phases of B/Co–2.

Effect of Temperature and Stabilizer Ratio on Hydrogen Generation

Figure 7 shows the effect of temperature (22, 40, and 60°C) and, stabilizer ratio (1, 5, 10, and 15 wt %) on hydrogen generation in the presence of B/Co–2 (catalyst/$NaBH_4$ wt ratio: 0.11). Increasing the reaction temperature the period needed to complete the hydrolysis reaction was changed. By increasing the NaOH content from 1 to 15 wt %, no functional increasing was observed in the hydrogen generation rate. Available free water needed for $NaBH_4$ hydrolysis, catalyst properties and, solubility of $NaBO_2$ reaction product in alkaline water effect the hydrogen generation rate. Accordingly, the highest rate of hydrogen production was observed at 1 and 5 wt % NaOH at 22°C. At a reaction temperature of 22°C, in 1 and

5 wt % NaOH solutions $NaBH_4$ hydrolysis proceeded with a higher rate and was completed in ≈100 min. Moreover, duration of the hydrolysis reaction conducted in the solution containing 10 and 15 wt % NaOH was ≈210 min. At 40°C in the solution with 10 wt % NaOH the shortest period for the hydrolysis reaction was observed. In addition, the reaction time varied from 25 to 60 min. At 60°C, the hydrolysis reaction was completed in ≈15 min and experiments with various NaOH concentrations indicated that the longest period was observed with 5 wt % NaOH.

Hydrogen Generation Kinetics

Table 4 gives the kinetic data obtained from assumption of zero-order, first-order and Langmuir–Hinshelwood kinetic model. As can be seen hydrogen generation data obeyed zero order kinetic model with 0.98 ± 1 coloration cofactor for all conditions. This means that reaction rate is independent on $NaBH_4$ concentration in all solutions containing NaOH. Also it can be easily seen from Table 4 first-order reaction model does not fit well for the behavior of hydrogen generation in the presence of B/Co–2. Zero-order kinetic model generally explains the high temperature systems and first-order kinetic model describes the low temperature systems [20].

In literature, Langmuir–Hinshelwood kinetic model generally used to explain the feature of catalytic reactions, also our kinetic modelling results fit for this model as can be seen from Table.4. Adsorption constant, K_a, was determined for different wt % NaOH concentrations by minimizing the function (Fig. 9). It was recognized that NaOH concentration affects the adsorption of reactant on catalysts surface according to Fig. 9. For different stabilizer—NaOH concentrations (1, 5, 10 and, 15 wt %) K_a values were determined as being 0.55, 0.342, 0.371 and, 0.205 L $mmol^{-1}$, respectively. These values show that by increasing the stabilizer concentration in reaction medium, it is possible to decrease adsorption of $NaBH_4$ and water over the B/Co–2 catalysts. In our hydrogen generation test, water was used in excess amounts so its concentration was accepted as constant and $NaBH_4$ was a rate-limiting reactant. After determining the adsorption value for the conditions used, Langmuir–Hinshelwood model was applied for all temperatures (22, 40 and, 60°C) and model shows good fitting for experimental data. This means that $NaBH_4$ and water molecules are adsorbed on the surface of the Co based catalyst. The hydrolysis mechanism of $NaBH_4$ over the non-noble metals surface sites have been reported by Andrieux et. al and, Kaufman and Sen. Andrieux suggested seven stages hydrolysis mechanism and Kaufman–Sen reported dissociative chemisorption of BH_4^- over metal active sites [21, 22].

Activation energy values of B/Co–2 catalysts in different mediums are shown in Table 5 and compared with previous data. These values were determined from the Arrhenius plot (Figs. 8–10). E_a values for zero-order and Langmuir–Hinshelwood kinetic model were determined to be approximately the same same (Table 5). NaOH concentration of $NaBH_4$ solution affects kinetic results of hydrolysis reaction by the co-precipitation Co–B catalyst. For instance, for the hydrolysis reaction conducted in $NaBH_4$ solution containing 10 and 15 wt % NaOH values of E_a and k are about the same. On the other hand, the reaction rate of hydrolysis conducted in a 10 wt % NaOH solution is two times higher than that performed in a 15 wt % NaOH solution. E_a values of zero order kinetic model were calculated to be 51.37, 43.55, 75.07 and, 73.18 kJ mol^{-1} for 1, 5, 10 and, 15 wt % NaOH and also k_0 were determined as being 14.18, 11.00, 23.29 and, 22.29 min^{-1}, respectively. E_a values can be compared with the previously reported data: 64.87 kJ mol^{-1} for amorphous Co–B catalyst [5], 77.96 kJ mol^{-1} for in situ prepared Co_2B [25] and, 49.60 kJ mol^{-1} for Co–Cu–B catalyst [26].

CONCLUSIONS

In this study, the use of H_3BO_3 and B_2O_3 for cobalt-boron catalysts co-precipitation synthesis and catalytic activities in hydrogen generation was investigated for the first time. While $CoSO_4$ and $Co(NO_3)_2$ salts were used with H_3BO_3 and B_2O_3, the Co–B catalyst with a crystalline structure was not obtained. Calcination temperatures above 500°C were necessary to synthesize Co based catalysts from $CoSO_4$, $Co(NO_3)_2$ salts in combination with H_3BO_3 and B_2O_3 using co-precipitation method. For this reason we recommended the use of $CoCl_2$ salt with H_3BO_3 and especially B_2O_3 as a boron sources for the co-precipitation method. A value of 0.11 wt/wt for the catalyst/$NaBH_4$ ratio is sufficient to achieve an efficient rate of hydrogen production in an alkaline $NaBH_4$ solution. It was found that an inexpensive Co–B catalyst, synthesized by co-precipitated B_2O_3 with $CoCl_2$, was catalytically active in $NaBH_4$ hydrolysis. Rate equation of hydrogen generation can be exemplified for 1 wt % NaOH alkaline $NaBH_4$ solution as given below.

$$-r_{NaBH_4} = 14.18e^{-51.37/RT}.$$

REFERENCES

1. Yang, C.C., Chen, M.S., and Chen, Y.W., *Int. J. Hydrogen Energy,* 2011, vol. 36, no. 2, p. 1418.
2. Santos, D.M.F. and Sequeira, C.A.C., *Renewable Sustainable Energy Rev.,* 2011, vol. 15, p. 3980.
3. Umegaki, T., Yan, J.M., Zhang, X.B., Shioyama, H., Kuriyama, N., and Xu, Q., *Int. J. Hydrogen Energy*, 2009, vol. 34, p. 2303.

4. Liu, C.H., Wua, Y.C., Chou, C.C., Chen, B.H., Hsueh, C.L., Ku, J.R., and Tsau, F., *Int. J. Hydrogen Energy*, 2012, vol. 37, p. 2950.
5. Jeong, S.U., Kim, R.K., Cho, E.A., Kim, H.J., Nam, S.W., Oh, I.H., Hong, S.A., and Kim, S.H., *J. Power Sources*, 2005, vol. 144, p. 129.
6. Amendola, S.C., Sharp-Goldman, S.L., Janjua, M.S., Spencer, N.C., Kelly, M.T., Petillo, P.J., and Binder, M., *Int. J. Hydrogen Energy,* 2000, vol. 25, p. 969.
7. Retnamma, R., Novais, A.Q., and Rangel, C.M., *Int. J. Hydrogen Energy*, 2011, vol. 36, p. 9772.
8. Akdim, O., Demirci, U.B., Muller, D., and Miele, P., *Int. J. Hydrogen Energy*, 2009, vol. 34, p. 2631.
9. Khan, R., Kim, S.W., Kim, T.J., and Nam, C.M., *Mater. Chem. Phys.*, 2008, vol. 112, p. 167.
10. Shen, X., Dai, M., Gao, M., Zhao, B., and Ding, W., *Chin. J. Catal.,* 2013, vol. 34, p. 979.
11. Hung, A.J., Tsai, S.F., Hsu, Y.Y., Ku, J.R., Chen, Y.H., and Yu, C.C., *Int. J. Hydrogen Energy*, 2008, vol. 33, p. 6205.
12. Fogler, S., *Elements of Chem. Reaction Engineering*, New Jersey: Prentice-Hall, 1999, 3rd ed.
13. Levenspiel, O., *Chem. Reaction Engineering,* New York: Wiley, 1999, 3rd ed.
14. Ozerova, A.M., Simagina, V.I., Komova, O.V., Netskina, O.V., Odegova, G.V., Bulavchenko, O.A., and Rudina, N.A., *J. Alloys Compd.*, 2012, vol. 513, p. 266.
15. Kantürk Figen, A. and Coşkuner, B., *Int. J. Hydrogen Energy*, 2013, vol. 38, no. 6, p. 2824.
16. Kantürk Figen, A., Coşkuner, B., Pişkin, M.B., and Özdemir Dere, Ö., *J. Int. Sci. Publ.: Mater., Met.*, 2013, vol. 7, no. 1, p. 43.
17. Coşkuner, B., Kantürk Figen, A., and Pişkin, S., *Reac. Kinet. Mech. Catal.*, 2013, vol. 109, no. 2, p. 375.
18. Fernandes, R., Patel, N., Miotello, A., and Filippi, M., *J. Mol. Catal. A: Chem.,* 2009, vol. 298, p. 1.
19. Cavaliere, S., Hannauer, J., Demirci, U.B., Akdim, O., and Miele, P., *Catal. Today*, 2011, vol. 170, p. 3.
20. Garron, A., Świerczyński, D., Bennici, S., and Auroux, A., *Int. J. Hydrogen Energy*, 2009, vol. 34, p. 1185.
21. Andrieux, J., Demirci, U.B., and Miele, P., *Catal. Today*, 2011, vol. 170, p. 13.
22. Kaufman, C.M. and Sen, B., *J. Chem. Soc., Dalton Trans.*, 1985, p. 307.
23. Chamoun, R., Demirci, U.B., Zaatar, Y., Khoury, A., and Miele, P., *Int. J. Hydrogen Energy*, 2010, vol. 35, p. 6583.
24. Zhao, J., Ma, H., and Chen, J., *Int. J. Hydrogen Energy*, 2007, vol. 32, p. 4711.
25. Krishnan, P., Advani, S.G., and Prasad, A.K., *Int. J. Hydrogen Energy*, 2008, vol. 33, p. 7095.
26. Ding, X.L., Yuan, X., Jia, C., and Ma, Z.F., *Int. J. Hydrogen Energy*, 2010, vol. 35, p. 1107.